

Toward High Performance Computing of Compressible Flows using Lattice Boltzmann Method

Gabriel Nastac

Robert Tramel

Kord Technologies, Inc.

Advanced Modeling & Simulation Seminar Series

NASA Ames Research Center

August 23, 2018

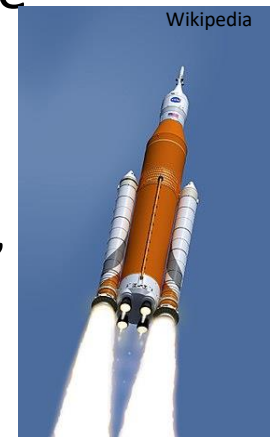


- Founded in 2008 in Huntsville, AL
- Employs over 250 personnel throughout the US
- Kord supports efforts by:

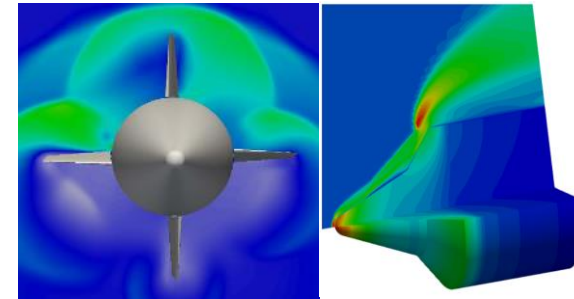
- US Army
- US Navy
- US Airforce
- MDA
- DHS
- NASA
- SMDC



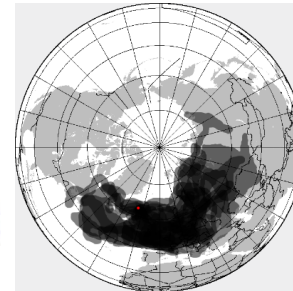
- Offers wide range of services including Systems Engineering, IT, Threat Systems Analysis, CFD, Software Engineering, Optical Engineering, and Project Management.
- Kord also supports Boeing on SLS in thermal analysis, stress analysis, fracture modeling, design engineering, and CFD



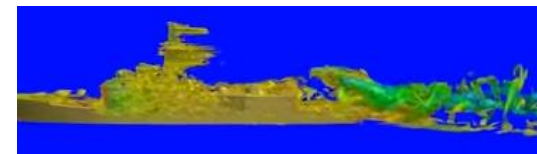
- High Speed Aerodynamics
- High Speed Aerothermodynamics
 - Conjugate Heat Transfer
 - Tightly Coupled Fluid-Structure Interactions
- Cryogenic Propellant Systems
 - Ascent Venting (AV) Models
- Shock Capturing Schemes (HLLC++)
 - NASA OVERFLOW
 - DoD Kestrel/Helios
- Rotorcraft Turbulence
 - Consistent LES
 - Low-Artificial Dissipation Algorithms
- Volcanic Ash Deposition in GT Engines
- Solvers:
 - In-House Unstructured and Structured Compressible NS
 - Government (DoD, NASA)
 - Commercial (ANSYS Fluent)
- Hardware:
 - In-house cluster
 - Government HPC resources



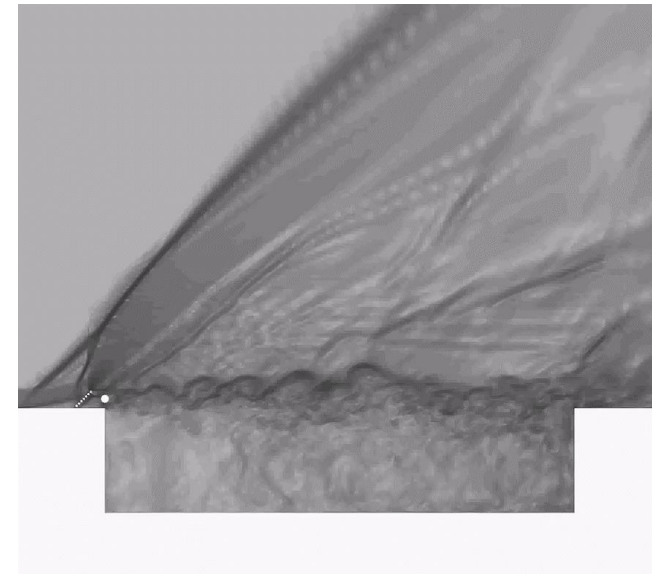
Aerodynamics/Aerothermodynamics



Map of volcanic ash cloud from the eruption of Eyjafjallajökull (red dot) in April 2010 [Met Office, 2017].



Helicopter Landing in Ship Airwake¹



Turbulence / Shock Waves / Acoustics

¹Coupled Flight Simulator and CFD Calculations of Ship Airwake using HPCMP CREATE™—AV Kestrel. Forsythe, et al. 2015



- Motivation
- Boltzmann Equation
- Low-Mach Lattice Boltzmann Method (LBM)
- Existing Low-Mach LBM Results
- LBM extensions to transonic and supersonic flows
- Upcoming Work and Preliminary 2D Results
- Future Work

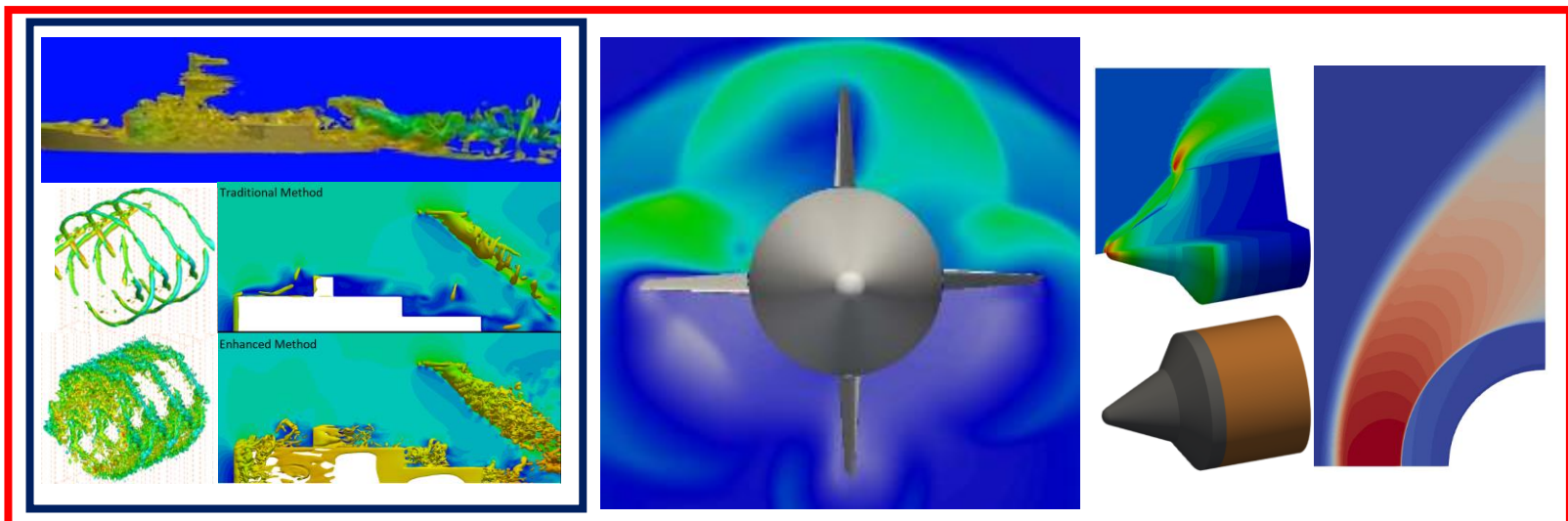
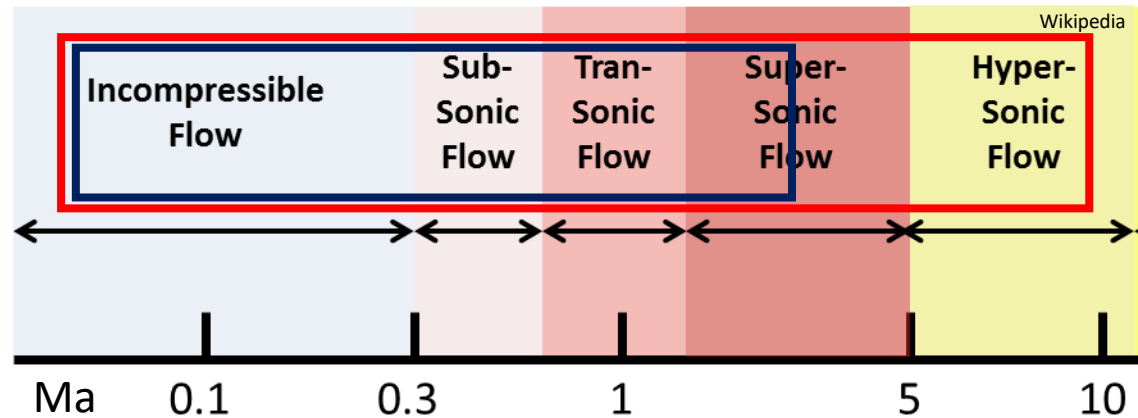
Motivation (1/3)

Solve Our Problems

Flows we are interested in

Flows where we think LBM can be utilized today

- LBM Benefits**
- Excellent Advection
 - Low Numerical Dissipation
 - Local Operations



Rotorcraft Aerodynamics

Top: Helicopter Landing in Ship Airwake¹

Bottom: Vortex Preserving and Consistent LES Algorithms

High Speed Aerodynamics

High Speed Aerothermodynamics

Monolithic CHT and TC FSI

¹Coupled Flight Simulator and CFD Calculations of Ship Airwake using HPCMP CREATE™—AV Kestrel. Forsythe, et al. 2015

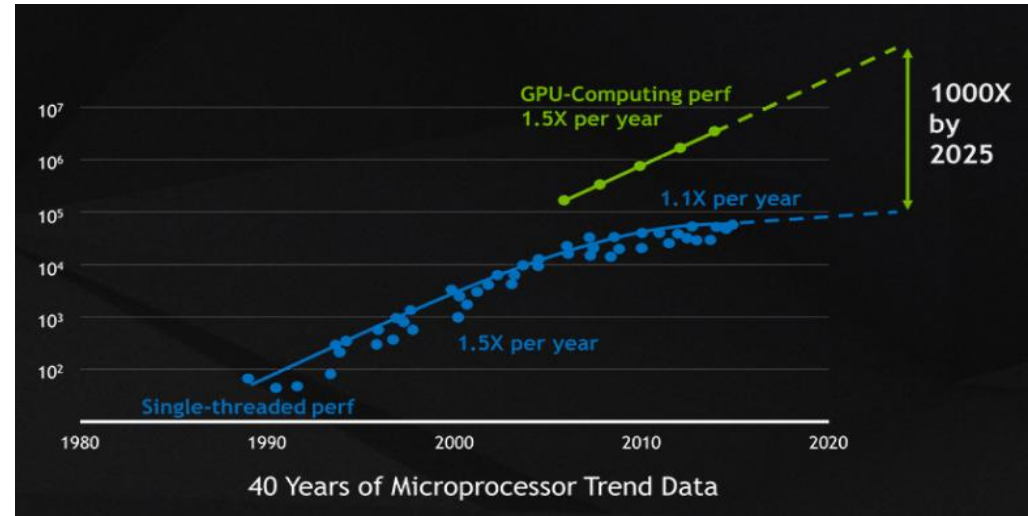
Effectively utilize current and future parallel architecture

Intel

Year	CPU Line	Max C/T
2017	Skylake-SP	28/56
2030	?	?

AMD

Year	CPU Line	Max C/T
2017	EPYC Naples	32/64
2019	EYPC Milan	48/96? 64/128?
2030	?	?



40 years of microprocessor data normalized to average processing power in 1980 [NVIDIA, 2018].

$$V = 0.44 \text{ m} \times 0.48 \text{ m} \times 0.83 \text{ m}$$

NVIDIA

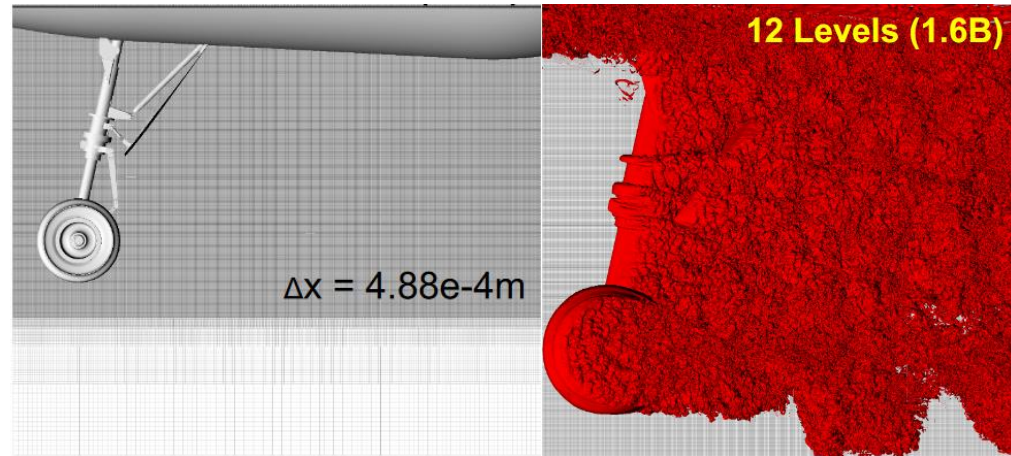
Year	Cluster	GPUs	GPU Memory [GB]	CUDA Cores	Single Precision [PFLOPS]	Deep Learning [PFLOPS]	Cost [\$1000]
2016	DGX-1	8 Tesla P100	128	28672	0.085	-	129
2018	DGX-2	16 Tesla V100	512	81920	0.252	2	400
2030	?	?	?	?	?	?	?

Motivation (3/3)

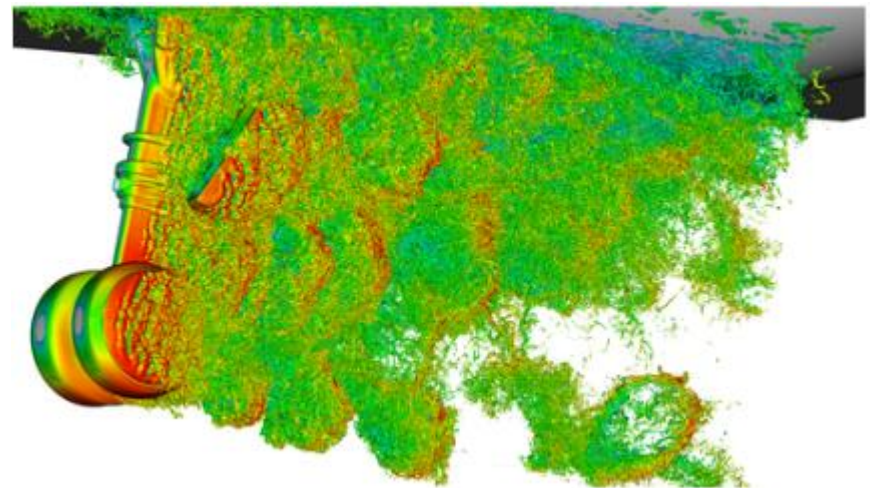
NASA LAVA Team Results



- Recent results by NASA LAVA show promise in the method for aerospace engineering analysis
- Massively parallel 3D Cartesian AMR Simulations
- Shown to dramatically reduce computational costs due to run-time and mesh generation
- Low numerical dissipation which paves way to higher fidelity LES
- Existing implementation is Low-Mach LBM
- Literature currently exists on extension of LBM to compressible flows - what is the efficiency of the method for compressible flows compared to existing solutions?



Low-Mach LBM of Landing Gear
[Barad, Kocheemoolayil, Kiris , 2018].



Vorticity colored by Mach number.
[Barad, Kocheemoolayil, Stich, Kiris, 2018].

- Density Distribution Function:

$$f(\mathbf{x}, \boldsymbol{\xi}, t)$$

- Macroscopic variables are moments of the distribution function, e.g.:

$$\rho(\mathbf{x}, t) = \int f(\mathbf{x}, \boldsymbol{\xi}, t) d^3 \boldsymbol{\xi}$$

$$\rho(\mathbf{x}, t) \mathbf{u}(\mathbf{x}, t) = \int \boldsymbol{\xi} f(\mathbf{x}, \boldsymbol{\xi}, t) d^3 \boldsymbol{\xi}$$

$$\rho(\mathbf{x}, t) E(\mathbf{x}, t) = \frac{1}{2} \int |\boldsymbol{\xi}|^2 f(\mathbf{x}, \boldsymbol{\xi}, t) d^3 \boldsymbol{\xi}$$

- Evolution of f in time given by Boltzmann Equation:

$$\frac{df(\mathbf{x}, \boldsymbol{\xi}, t)}{dt} = \frac{\partial f}{\partial t} + \xi_j \frac{\partial f}{\partial x_j} + \frac{F_j}{\rho} \frac{\partial f}{\partial \xi_j} = \Omega(f(\mathbf{x}, \boldsymbol{\xi}, t))$$



- \mathcal{H} -Theorem originally introduced by Boltzmann in 1872:

$$\mathcal{H}(f) = \int f \ln f \, d^3 \xi$$

- The \mathcal{H} -Theorem is directly related to entropy density:

$$\rho_s = -R\mathcal{H}$$

- Boltzmann showed that the quantity \mathcal{H} can only decrease and reaches a minima at equilibrium (in other words, equilibrium occurs at maximum entropy).
- Collisions drive the density distribution function towards equilibrium.



- The collision operator represents the non-linear local redistribution of f due to collisions.
- The operator conserves mass, momentum, and energy (elastic):

$$\begin{aligned}\int \Omega(f) d^3 \xi &= 0 \\ \int \xi \Omega(f) d^3 \xi &= \mathbf{0} \\ \int |\xi|^2 \Omega(f) d^3 \xi &= 0\end{aligned}$$

- The Bhatnagar-Gross-Krook (BGK) operator [Bhatnagar, 1954] is given as a relaxation towards equilibrium (Maxwell-Boltzmann Distribution):

$$\Omega(f) = -\frac{1}{\tau} (f - f^{eq})$$

- We first develop a velocity distribution lattice:

$$\frac{\partial f}{\partial t} + \xi_j \frac{\partial f}{\partial x_j} = \Omega(f) \rightarrow \frac{\partial f_i}{\partial t} + \xi_{ij} \frac{\partial f_i}{\partial x_j} = \Omega_i(f)$$

- At each point, we now have a lattice of dimension $DdQn$, where d is the dimension and n is the number of lattice velocities
- We have a hyperbolic ODE which we can simplify using MOC:

$$f_i(\mathbf{x} + \boldsymbol{\xi}_i, t + 1) - f_i(\mathbf{x}, t) = \Omega_i(f_i(\mathbf{x}, t))$$

$$\boldsymbol{\xi}_4 = \overset{f_4}{(-1, 1)}$$

$$\boldsymbol{\xi}_3 = \overset{f_3}{(0, 1)}$$

$$\boldsymbol{\xi}_2 = \overset{f_2}{(1, 1)}$$

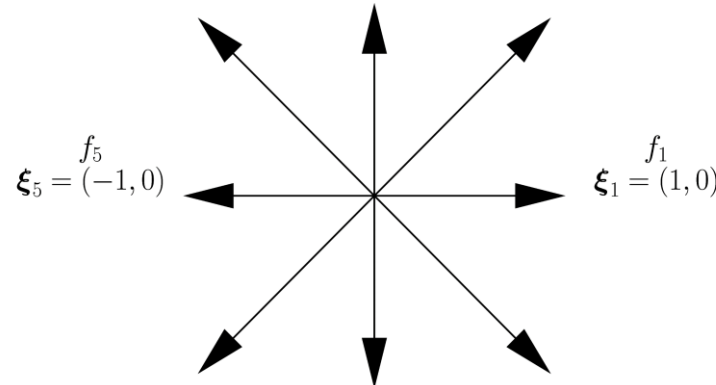
$$\boldsymbol{\xi}_5 = \overset{f_5}{(-1, 0)}$$

$$\boldsymbol{\xi}_1 = \overset{f_1}{(1, 0)}$$

$$\boldsymbol{\xi}_6 = \overset{f_6}{(-1, -1)}$$

$$\boldsymbol{\xi}_7 = \overset{f_7}{(0, -1)}$$

$$\boldsymbol{\xi}_8 = \overset{f_8}{(1, -1)}$$



D2Q9 lattice with outer distribution values and lattice velocities.

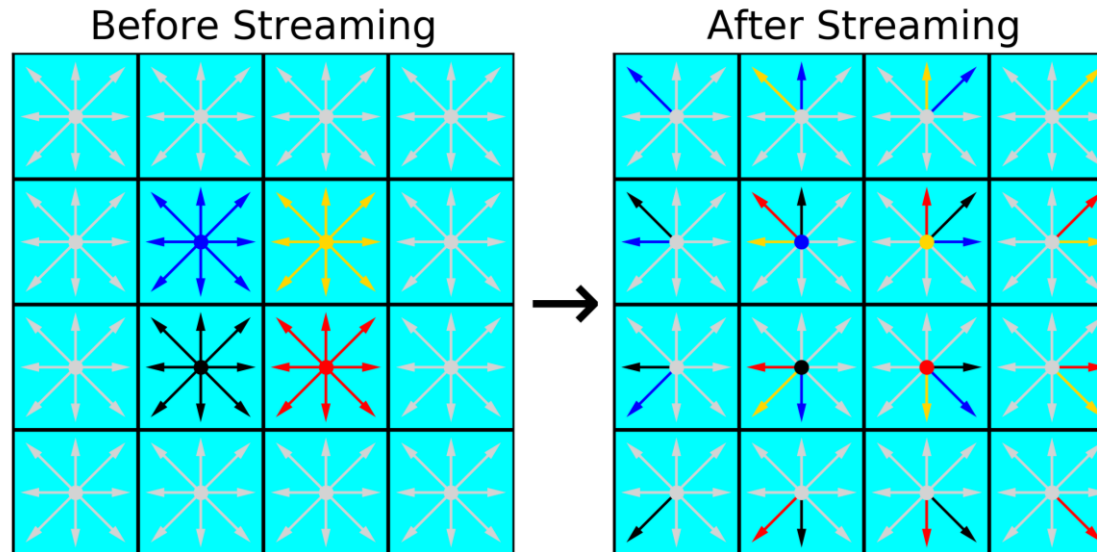
$$f_i(\mathbf{x} + \boldsymbol{\xi}_i, t + 1) - f_i(\mathbf{x}, t) = \Omega_i(f_i(\mathbf{x}, t))$$

- The above equation is two main steps: collision and streaming
- Collision:

$$f'_i(\mathbf{x}, t) = f_i(\mathbf{x}, t) + \Omega_i(f_i(\mathbf{x}, t))$$

- Streaming:

$$f_i(\mathbf{x} + \boldsymbol{\xi}_i, t + 1) = f'_i(\mathbf{x}, t)$$



Streaming step of Lattice Boltzmann for D2Q9 Lattice.
The inner four cells are consistently colored to visualize the propagation.

$$\Omega(f) = -\frac{1}{\tau}(f - f^{eq}) \rightarrow \Omega_i(f_i) = -\frac{1}{\tau}(f_i - f_i^{eq})$$

- What is the equilibrium distribution, f_i^{eq} ? The continuous equilibrium distribution is the Maxwell-Boltzmann distribution. The discrete form is developed by discretizing the continuous velocity space. The moments of interest must be conserved¹.

$$f^{eq}(\rho, \mathbf{u}, \boldsymbol{\xi}) = \frac{\rho}{(2\pi)^{\frac{3}{2}}} \exp\left[-\frac{(\boldsymbol{\xi} - \mathbf{u})^2}{2}\right]$$

- Low-Mach Equilibrium distribution (c_s is particle speed, W_i are lattice weights):

$$f_i^{eq} = W_i \rho \left(1 + \frac{\boldsymbol{\xi}_i \cdot \mathbf{u}}{c_s^2} + \frac{(\boldsymbol{\xi}_i \cdot \mathbf{u})^2}{2c_s^4} - \frac{|\mathbf{u}|^2}{2c_s^2} \right)$$

- Macroscopic variables can be computed based on existing distribution values:

$$\rho = \sum_{i=1}^n f_i = \sum_{i=1}^n f_i^{eq}$$

$$\rho \mathbf{u} = \sum_{i=1}^n \boldsymbol{\xi}_i f_i = \sum_{i=1}^n \boldsymbol{\xi}_i f_i^{eq}$$

- The relaxation time is a function of the viscosity.

- Multiple methods in literature can be used to determine macroscopic governing equations
- Chapman-Enskog expansion (1910~1920) is a popular approach and commonly used.
- Essentially a linearization of Boltzmann distribution based on the Knudsen number:

$$Kn = \frac{\lambda}{L} \sim \epsilon$$

$$f_i = f_i^{eq} + \epsilon f_i^{(1)} + \epsilon^2 f_i^{(2)} + \dots$$

- It can be shown that the method described thus far recovers the unsteady isothermal weakly compressible (essentially incompressible) Navier-Stokes equations with $\mathcal{O}(Ma^2)$ error:

$$\partial_t (\rho) + \partial_j (\rho u_j) = 0$$

$$\partial_t (\rho u_i) + \partial_j (\rho u_i u_j + \delta_{ij} p - 2\mu S_{ij}) = 0$$

Benefits

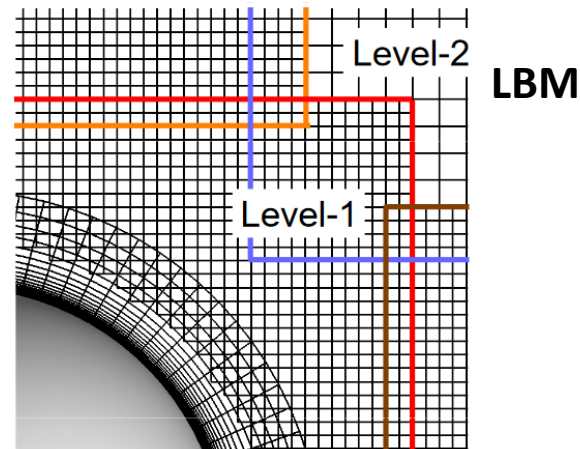
- No Poisson equation – a bottleneck in typical incompressible NS solvers
- Simple explicit algorithm
- Collisions are entirely local
- Essentially perfect advection by construction
- Low-Numerical Dissipation

Downsides

- The error terms are of $\mathcal{O}(Ma^2)$ → extensions must be done to simulate compressible flow ($Ma \geq 0.3$)
- Prandtl number, $Pr = 1$
- Method is based on translational energy modes (monatomic gases) and consequently the specific heat ratio is fixed ($\gamma = 5/3$ for 3D)
- Unsteady by construction
- Resolving wall is prohibitive with Cartesian AMR → Wall Models or Dual-Mesh

Dual-Mesh
(DoD CREATE-AV Kestrel/Helios)

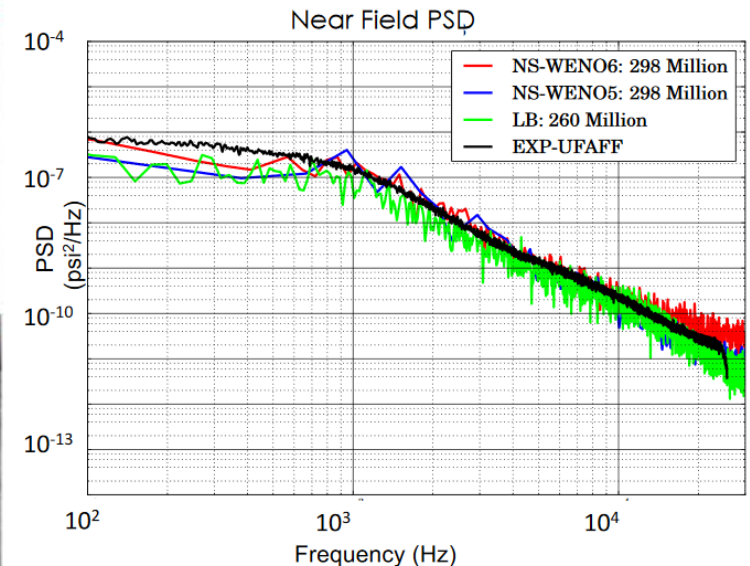
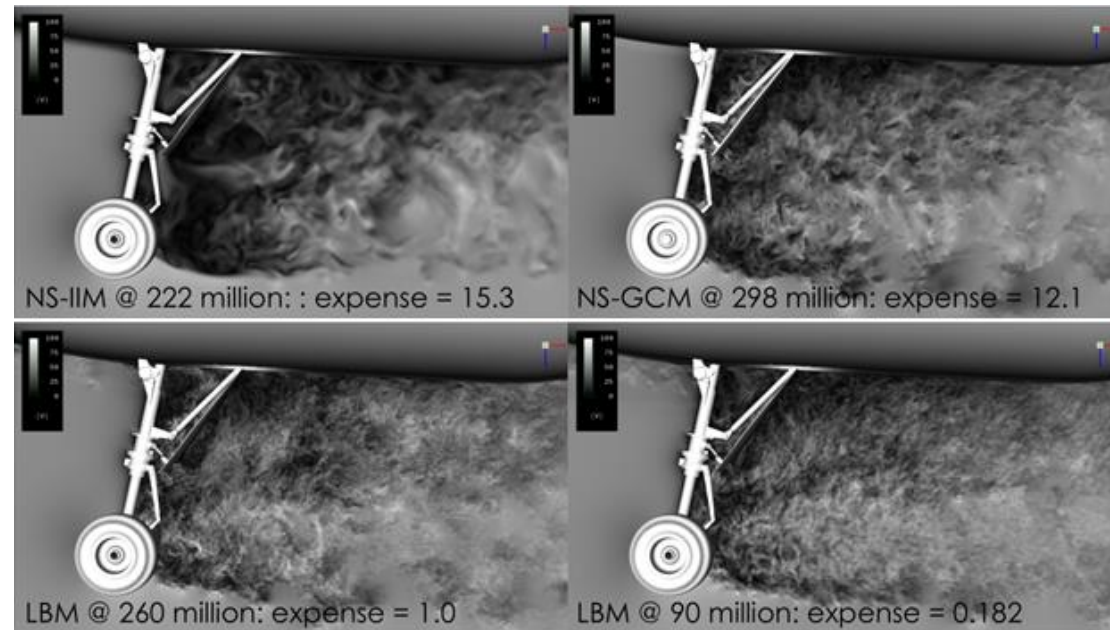
NS



Method	CPU Cores (type)	Cells (million)	Wall Days to 0.19 seconds	Core Days to 0.19 seconds	Relative SBU Expense
NS-GCM	3000 (ivy)	298	20.5	61352	12.1
NS-IIM	9600 (has)	222	6.1	58490	15.3
LBM	1400 (bro)	260	2.25	3156	1

GCM: Ghost Cell Method

IIM: Immersed Interface Method



[Barad, Kocheemoolayil, Kiris , 2018]

Unoptimized LBM with 1.6 billion cells 2~ faster than NS with 300 million cells



- There are numerous research groups around the world working on compressible flow extensions to LBM
- The method which we think has the most promise currently is the Entropic Compressible LBM by N. Frapolli, S. S. Chikatamarla, and I. V. Karlin of ETH Zurich (2016)¹
- Key components of the method:
 - Unconditionally stable (enables high Re simulations)
 - Increases Mach number limit by an order of magnitude (up to 3.0)
 - Variable Prandtl number and Specific Heat Ratio (e.g. $Pr = 0.71$, $\gamma = 1.4$ for standard air)
 - Entropic component adds artificial dissipation for shock capturing without sensors
- Method was tested and validated on 2D and 3D geometry using AMR¹:
 - 2D Inviscid/Viscous Transonic & Supersonic NACA0012
 - 3D Inviscid Onera M6 Wing
 - 3D Compressible Homogeneous Isotropic Turbulence
- Potential issues of the method:
 - Computational Efficiency. How does the method compare to existing methods?
 - Entropic methods in general (including low-Mach) add artificial viscosity in under-resolved areas similar to sub-grid scale (SGS) LES models – not really an issue.



- Implement compressible LBM¹
- Simulate canonical 2D (e.g. TG, VC, oblique shock) and 3D (TG) test cases
- Validate and verify the implementation
- Benchmark against existing solvers (FUN3D, OVERFLOW)
- Determine scalability and performance using CPU MPI and NVIDIA's CUDA

¹N. Frapolli, S. S. Chikatamarla, and I. V. Karlin, Phys. Rev. E 93, 063302 (2016).

The Entropic Compressible LBM relies on three primary components:

- Enlarged lattice and temperature dependent lattice weights
- Boltzmann's \mathcal{H} -Theorem
- An additional set of populations (g) that represent rotational and vibrational energy to enable variable γ

Similarly to traditional LBM, this method uses a lattice. The standard method uses a DdQ7^d lattice ($0, \pm 1, \pm 2, \pm 3$), or D2Q49 and D3Q343 for 2D and 3D respectively.

Lattice pruning can be used to reduce 3D lattice to D3Q39.

Method has the same structure and solution technique as traditional LBM:

$$f_i(\mathbf{x} + \boldsymbol{\xi}_i, t + 1) - f_i(\mathbf{x}, t) = \Omega_f(f_i)$$

$$g_i(\mathbf{x} + \boldsymbol{\xi}_i, t + 1) - g_i(\mathbf{x}, t) = \Omega_g(f_i)$$

$$\Omega_f(f_i) = \alpha\beta_1(f_i^{eq} - f_i) + 2(\beta_1 - \beta_2)(f_i^* - f_i^{eq})$$

$$\Omega_g(f_i) = \alpha\beta_1(g_i^{eq} - g_i) + 2(\beta_1 - \beta_2)(g_i^* - g_i^{eq})$$

$$\begin{aligned}
 w_0 &= w_0(T) \\
 w_{\pm 1} &= w_{\pm 1}(T) \\
 w_{\pm 2} &= w_{\pm 2}(T) \\
 w_{\pm 3} &= w_{\pm 3}(T)
 \end{aligned}$$

$$W_i(\xi_{ix}, \xi_{iy}, \xi_{iz}, T) = w_{ix}w_{iy}w_{iz}$$

$$\sum_{i=1}^n W_i = 1$$

Discrete \mathcal{H} -Theorem

$$\mathcal{H}(f) = \int f \ln f \, d^3\xi \rightarrow \mathcal{H}(f) = \sum_{i=1}^n f_i \ln f_i/W_i$$

$$\rho = \sum_{i=1}^n f_i = \sum_{i=1}^n f_i^{eq}$$

$$\rho \mathbf{u} = \sum_{i=1}^n \xi_i f_i = \sum_{i=1}^n \xi_i f_i^{eq}$$

$$2\rho E^{tr} = 2\rho DT + \rho |\mathbf{u}|^2 = \sum_{i=1}^n |\xi_i|^2 f_i = \sum_{i=1}^n |\xi_i|^2 f_i^{eq}$$

$$2\rho E = 2\rho C_v T + \rho |\mathbf{u}|^2 = \sum_{i=1}^n |\xi_i|^2 f_i + \sum_{i=1}^n g_i = \sum_{i=1}^n |\xi_i|^2 f_i^{eq} + \sum_{i=1}^n g_i^{eq}$$

- Translational energy and total energy are both tracked
- Rotational energy is tracked using the separate distributions g_i

Minimize \mathcal{H} using LM to enforce conservation to obtain f_i^{eq} :

$$J(f_i^{eq}, \chi, \zeta, \lambda) = \sum_{i=1}^n f_i^{eq} \ln f_i^{eq} / W_i + \chi \left(\rho - \sum_{i=1}^n f_i^{eq} \right) + \zeta \cdot \left(\rho \mathbf{u} - \sum_{i=1}^n \xi_i f_i^{eq} \right) + \lambda \left(2\rho E^{tr} - \sum_{i=1}^n |\xi_i|^2 f_i^{eq} \right)$$

$$\frac{\partial J}{\partial f_i^{eq}} = 0 = \sum_{i=1}^n \left(\ln \frac{f_i^{eq}}{W_i} + 1 - \chi - \zeta \cdot \xi_i - \lambda |\xi_i|^2 \right)$$

An extremum is ensured with the following form of f_i^{eq} :

$$f_i^{eq} = \rho W_i \exp(\chi + \zeta \cdot \xi_i + \lambda |\xi_i|^2) \quad \leftarrow \text{Positive-Definite}$$

$$g_i^{eq} = (2C_v T - D) f_i^{eq}$$

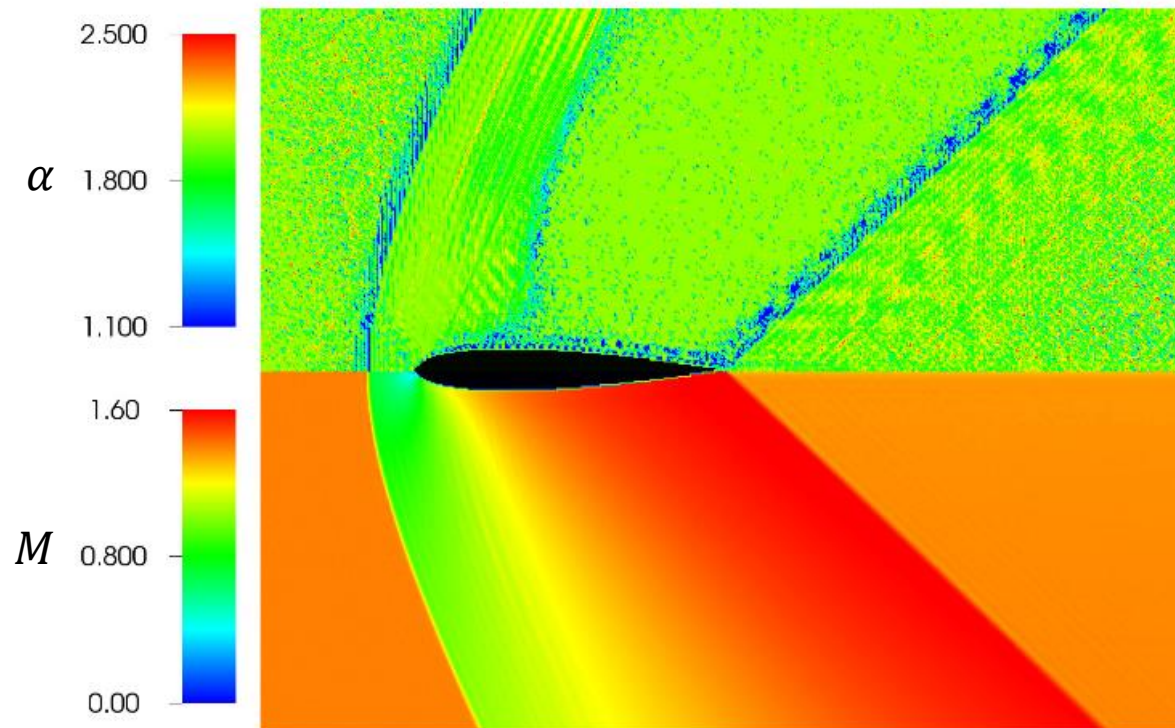
$$f^{eq}(\rho, \mathbf{u}, \xi, \theta) = \frac{\rho}{(2\pi\theta)^{\frac{3}{2}}} \exp \left[-\frac{(\xi - \mathbf{u})^2}{2\theta} \right] \quad \leftarrow \begin{array}{l} \text{Continuous Velocity Space} \\ \text{Maxwell-Boltzmann Distribution} \end{array}$$

5th order Hermite polynomial expansion

$$\begin{aligned}
 f_i^{eq} &= \rho W_i \left(1 + \xi_i \cdot \mathbf{u} + \frac{1}{2} [(\xi_i \cdot \mathbf{u})^2 - \mathbf{u} \cdot \mathbf{u}] + \frac{T-1}{2} (\xi_i \cdot \xi_i - D) + \frac{\xi_i \cdot \mathbf{u}}{6} [(\xi_i \cdot \mathbf{u})^2 - 3\mathbf{u} \cdot \mathbf{u}] \right. \\
 &+ \frac{T-1}{2} (\xi_i \cdot \mathbf{u})(\xi_i \cdot \xi_i - D - 2) + \frac{1}{24} [(\xi_i \cdot \mathbf{u})^4 - 6(\xi_i \cdot \mathbf{u})^2(\mathbf{u} \cdot \mathbf{u}) + 3(\mathbf{u} \cdot \mathbf{u})^2] \\
 &+ \frac{T-1}{4} [(\xi_i \cdot \xi_i - D - 2)((\xi_i \cdot \mathbf{u})^2 - \mathbf{u} \cdot \mathbf{u}) - 2(\xi_i \cdot \mathbf{u})^2] \\
 &+ \frac{(T-1)^2}{28} [(\xi_i \cdot \xi_i)^2 - 2(D+2)(\xi_i \cdot \xi_i) + D(D+2)] \\
 &+ \frac{\xi_i \cdot \mathbf{u}}{120} [(\xi_i \cdot \mathbf{u})^4 - 10(\xi_i \cdot \mathbf{u})^2(\mathbf{u} \cdot \mathbf{u}) + 15(\mathbf{u} \cdot \mathbf{u})^2] \\
 &+ \frac{T-1}{12} (\xi_i \cdot \mathbf{u}) [(\xi_i \cdot \xi_i - D - 4)((\xi_i \cdot \mathbf{u})^2 - 3(\mathbf{u} \cdot \mathbf{u})) - 2(\xi_i \cdot \mathbf{u})^2] \\
 &\left. + \frac{(T-1)^2}{8} (\xi_i \cdot \mathbf{u}) [(\xi_i \cdot \xi_i)^2 - D(D+4)(\xi_i \cdot \xi_i) + (D+2)(D+4)] \right)
 \end{aligned}$$

$$\mathcal{H}(f) = \mathcal{H}(f + \alpha(f^{eq} - f))$$

- Entropic estimate α is the non-trivial root of above constraint
- Entropy is guaranteed to remain the same or increase by construction
- For fully-resolved simulations, α tends to 2 which is the BGK value



NACA0012 Airfoil¹
 $M_{\infty} = 1.4, Re = 3 \times 10^6$

¹N. Frapolli, S. S. Chikatamarla, and I. V. Karlin, Phys. Rev. E 93, 063302 (2016).

- Relaxation parameters are functions of dynamic viscosity and thermal conductivity (e.g. Sutherland law for viscosity and Prandtl number to compute thermal conductivity)

$$\beta_1 = \frac{1}{\frac{2\mu}{\rho T} + 1}$$

$$\beta_2 = \frac{1}{\frac{2\kappa}{\rho C_p T} + 1}$$

$$\Omega_f(f_i) = \alpha\beta_1(f_i^{eq} - f_i) + 2(\beta_1 - \beta_2)(f_i^* - f_i^{eq})$$

$$\Omega_g(f_i) = \alpha\beta_1(g_i^{eq} - g_i) + 2(\beta_1 - \beta_2)(g_i^* - g_i^{eq})$$

$$f_i^* = f_i^{eq} + W_i \bar{Q} : R$$

$$R = \frac{\xi_i \otimes \xi_i \otimes \xi_i - 3T \xi_i I}{6T^3}$$

$$\bar{Q} = \sum_{i=1}^n f_i(\xi_i - \mathbf{u}) \otimes (\xi_i - \mathbf{u}) \otimes (\xi_i - \mathbf{u})$$

$$g_i^* = g_i^{eq} + W_i \bar{q} \cdot \mathbf{r}$$

$$\mathbf{r} = \frac{\xi_i}{T}$$

$$\bar{q} = \sum_{i=1}^n g_i(\xi_i - \mathbf{u})$$

- Chapman-Enskog expansion (1910~1920) is a popular approach and commonly used.
- Essentially a linearization of Boltzmann distribution based on the Knudsen number:

$$Kn = \frac{\lambda}{L} \sim \epsilon$$

$$f_i = f_i^{eq} + \epsilon f_i^{(1)} + \epsilon^2 f_i^{(2)} + \dots$$

- It can be shown that the method described thus far recovers the unsteady compressible Fourier-Navier-Stokes equations:

$$\partial_t (\rho) + \partial_j (\rho u_j) = 0$$

$$\partial_t (\rho u_i) + \partial_j (\rho u_i u_j + \delta_{ij} p + \tau_{ij}) = 0$$

$$\partial_t (\rho E) + \partial_j \left((\rho E + p) u_j + \tau_{ij} u_i + q_j \right) = 0$$

- Collision:

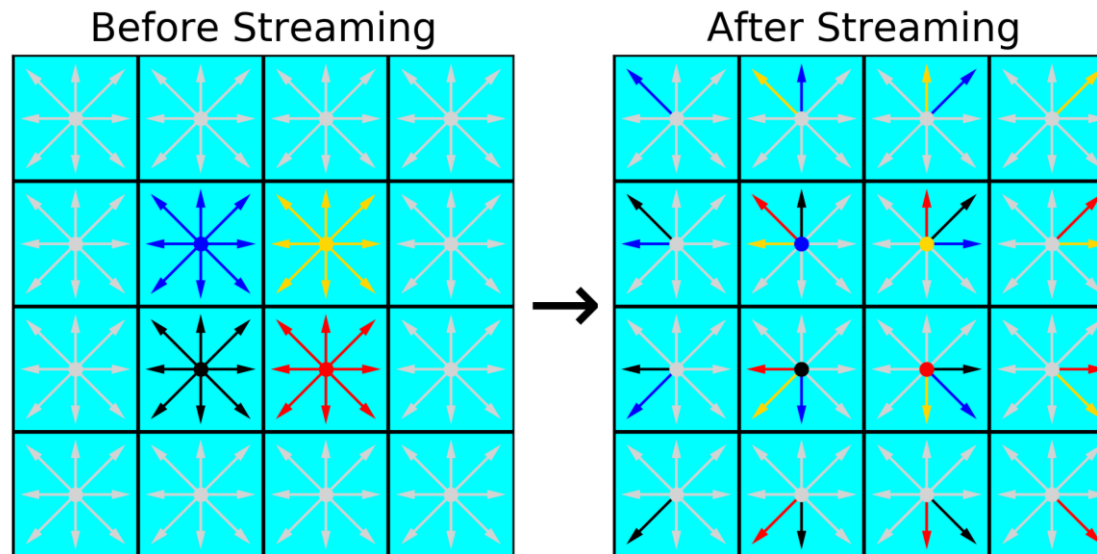
$$f'_i(\mathbf{x}, t) = f_i(\mathbf{x}, t) + \Omega_f(f_i(\mathbf{x}, t))$$

$$g'_i(\mathbf{x}, t) = g_i(\mathbf{x}, t) + \Omega_g(g_i(\mathbf{x}, t))$$

- Streaming:

$$f_i(\mathbf{x} + \boldsymbol{\xi}_i, t + 1) = f'_i(\mathbf{x}, t)$$

$$g_i(\mathbf{x} + \boldsymbol{\xi}_i, t + 1) = g'_i(\mathbf{x}, t)$$



Streaming step of Lattice Boltzmann for D2Q9 Lattice. The inner four cells are consistently colored to visualize the propagation.

Potential issues of the method:

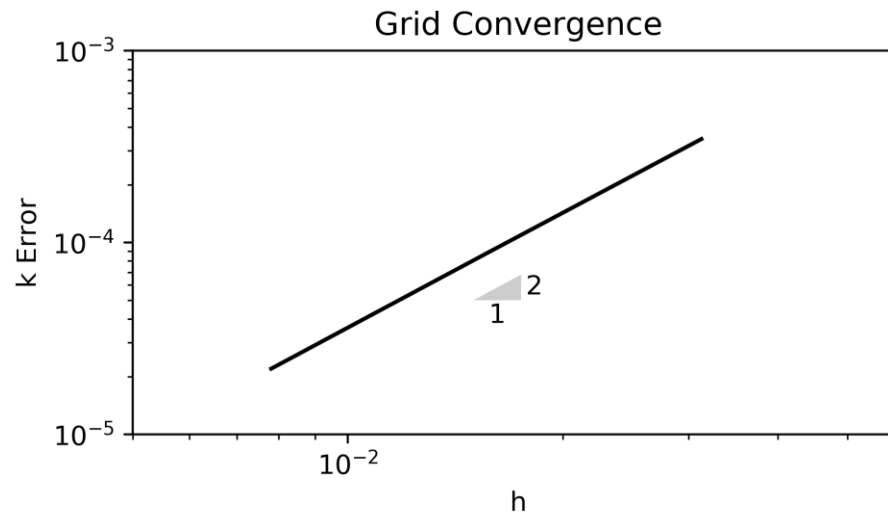
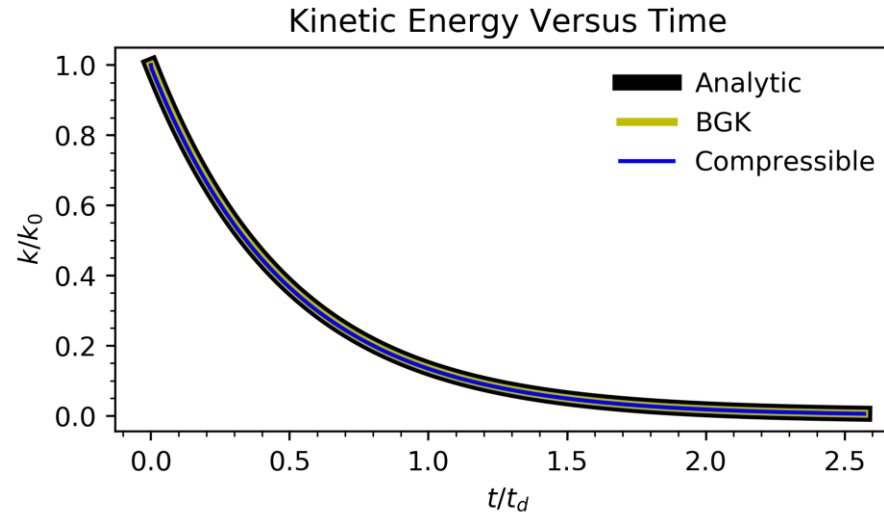
- Computational Efficiency. How does the method compare to existing methods?
- Entropic methods add artificial viscosity in under-resolved areas similar to sub-grid scale (SGS) LES models.

Method requires at each node at each timestep:

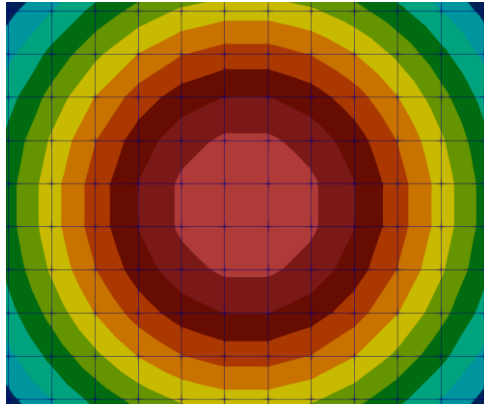
- a multi-dimensional non-linear solve for equilibrium
- a scalar non-linear solve for entropic constant, α

Our preliminary 2D results show that these non-linear solves are the bulk of the computational time.

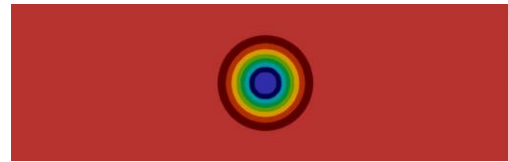
2D Taylor Green Vortex



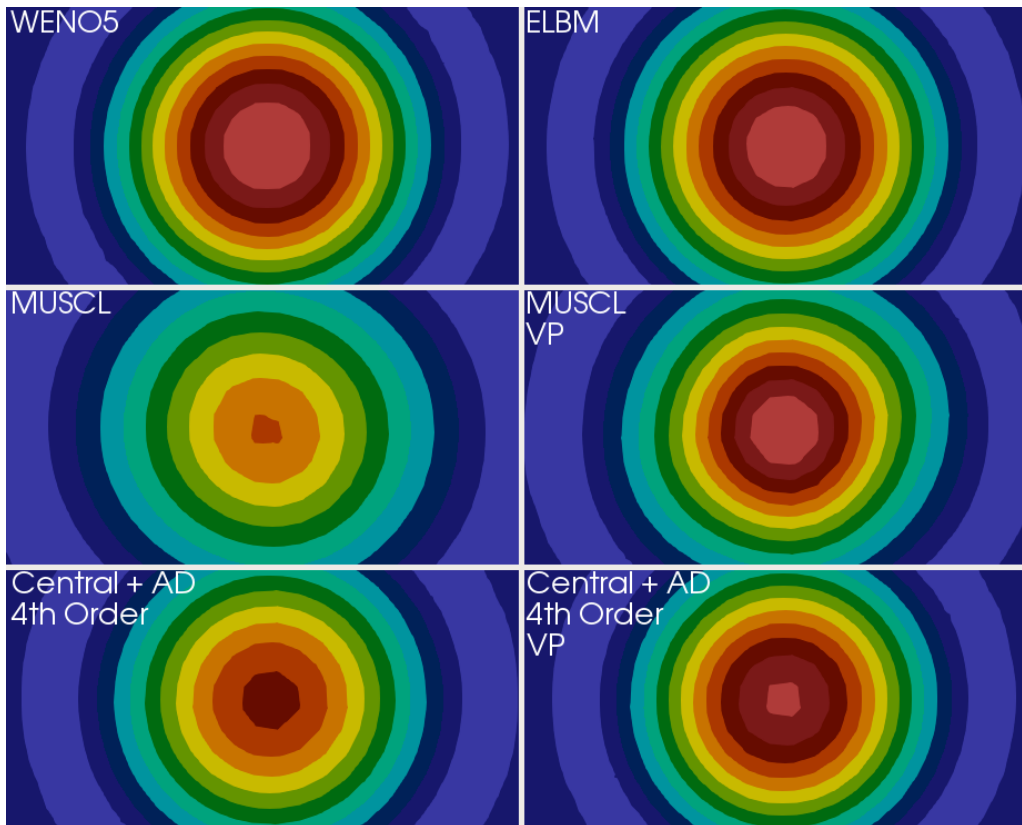
$t = 0$



2D Inviscid Vortex Convection
($M = 0.5$, 128^2 Grids, 5L Distance)



VP = Vortex Preserving (AVC)
AD = Artificial Dissipation



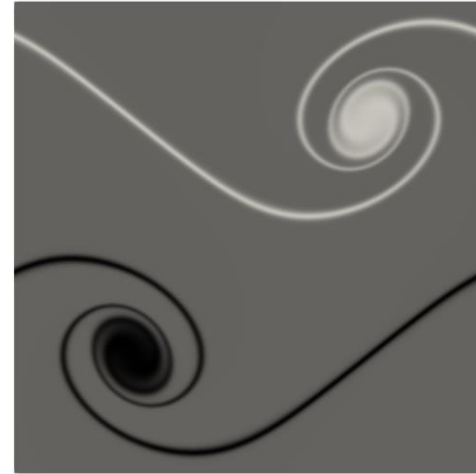
Method	$\frac{ \overline{\omega}_c }{ \overline{\omega}_{c0} }$ (%)
Analytic	100%
Roe-WENO5	99.8%
ELBM 2 nd Order	99.7%
Roe-MUSCL 3 rd Order	70.9%
Roe-MUSCL 3 rd Order VP	99.0%
Central+AD 4 th Order	80.5%
Central+AD 4 th Order VP	94.0%

Preliminary 2D Results

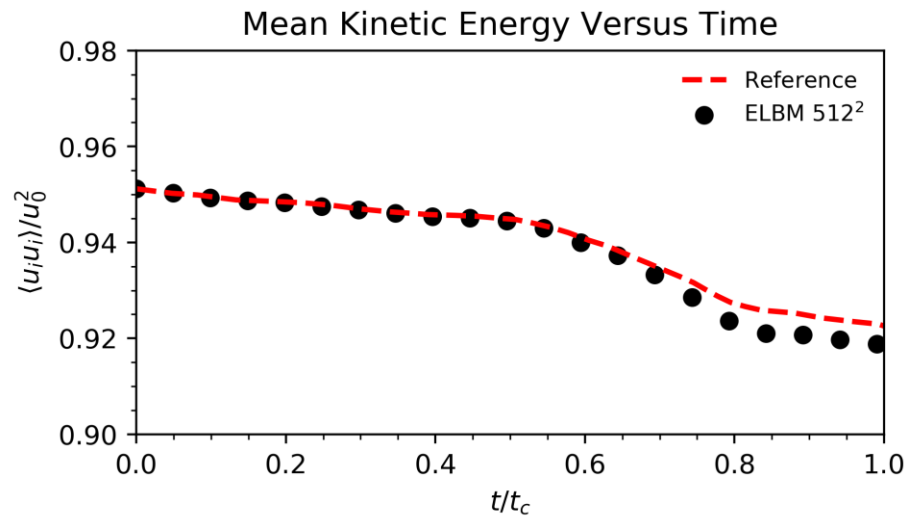
Double Shear Layer ($M = 0.35$ $Re = 30,000$)



$t_c = 0$

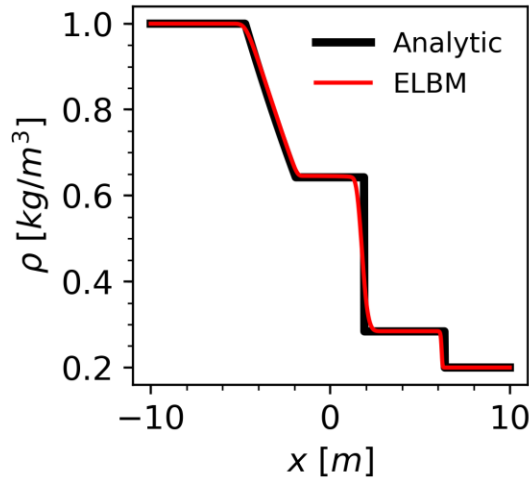


$t_c = 1$

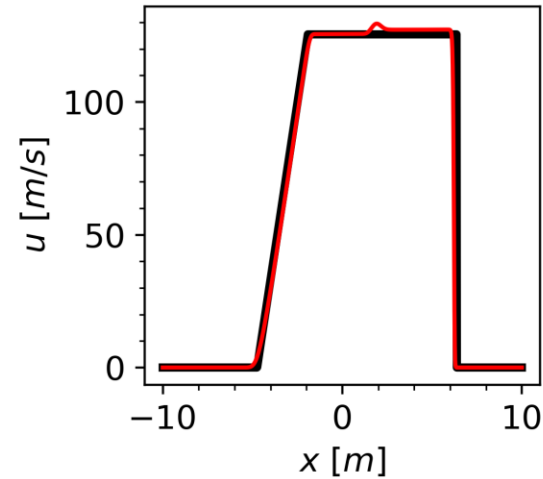


Shock Tube (1024x1 Grid)

Density



Velocity



$$\rho_L = 1.0 \frac{kg}{m^3}$$

$$\rho_R = 0.2 \frac{kg}{m^3}$$

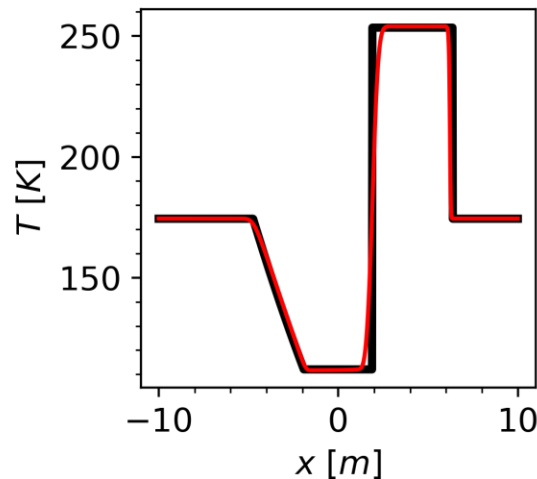
$$P_L = 50 \text{ kPa}$$

$$P_R = 10 \text{ kPa}$$

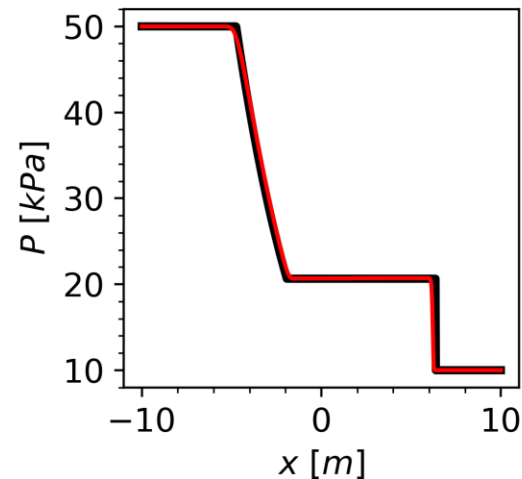
$$u_L = 0.0 \frac{m}{s}$$

$$u_R = 0.0 \frac{m}{s}$$

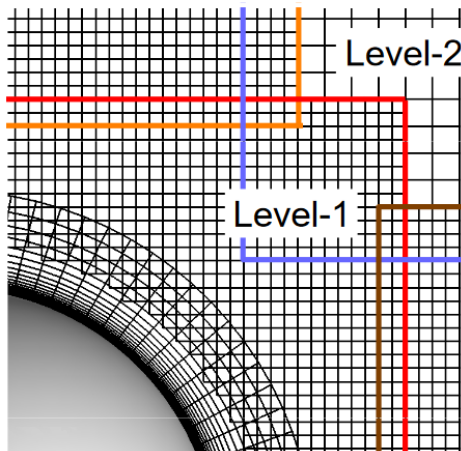
Temperature



Pressure

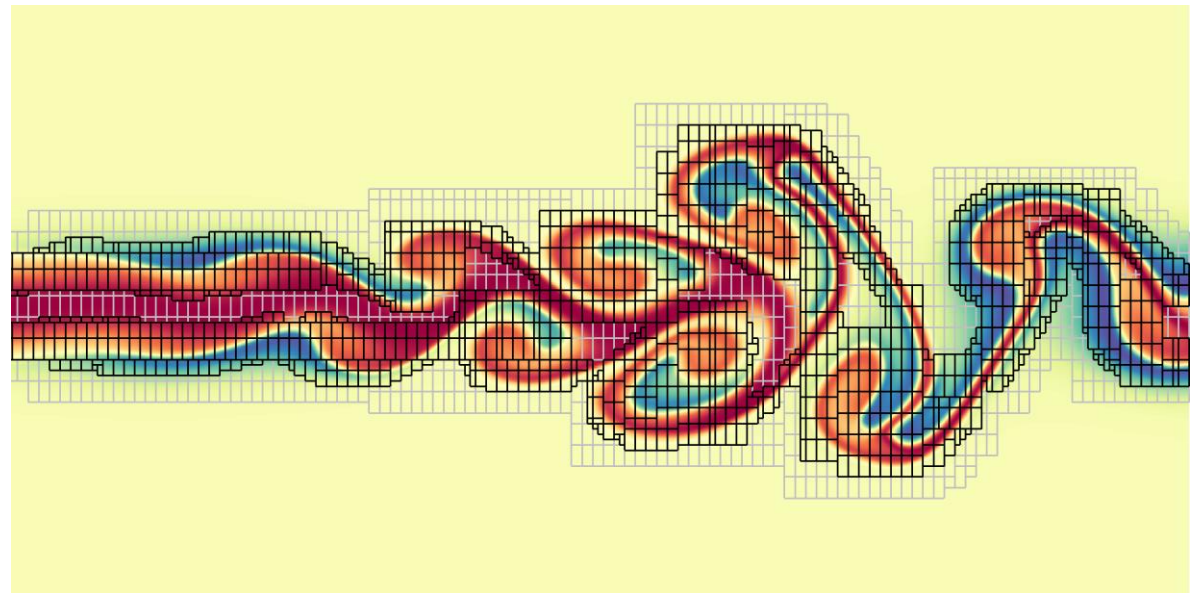


- Test transonic/supersonic cases
- Test 3D performance (3D TG/HIT/etc.)
- Extend implementation with Cartesian AMR framework:
 - Chombo
 - SAMRAI
 - AMReX
- Incorporate either wall-models or dual-mesh overset to enable complex geometry simulations



Dual-Mesh

(DoD CREATE-AV Kestrel/Helios)
OVERFLOW



Temperature field of a flame computed with RNS, a block-structured AMR solver that uses AMReX as a basis for grid generation and data structures. [AMReX, 2018].